Immunology
The Journal of cells, molecules, systems and technologies

British Society for immunology

IMMUNOLOGY ORIGINAL ARTICLE

Cachexia in the non-obese diabetic mouse is associated with CD4$^+$ T-cell lymphopenia

Chunfang Zhao, Zhuanzhi Wang, Michael W. Robertson and Joanna D. Davies

Torrey Pines Institute for Molecular Studies, General Atomics Court, San Diego, CA, USA

doi:10.1111/j.1365-2567.2008.02819.x
Received 13 November 2007; revised 8 January, 28 January 2008; accepted 28 January 2008.
Correspondence: J. D. Davies, Torrey Pines Institute for Molecular Studies, 3550 General Atomics Court, San Diego, CA 92121, USA.
Email: jdavies @tpims.org
Senior author: Joanna D. Davies

Summary

One of the long-term consequences of Type I diabetes is weight loss with muscle atrophy, the hallmark phenotype of cachexia. A number of disorders that result in cachexia are associated with immune deficiency. However, whether immune deficiency is a cause or an effect of cachexia is not known. This study examines the non-obese diabetic mouse, the mouse model for spontaneous Type I diabetes, as a potential model to study lymphopenia in cachexia, and to determine whether lymphopenia plays a role in the development of cachexia. The muscle atrophy seen in patients with Type I diabetes involves active protein degradation by activation of the ubiquitin–proteasome pathway, indicating cachexia. Evidence of cachexia in the non-obese diabetic mouse was determined by measuring skeletal muscle atrophy, activation of the ubiquitin–proteasome pathway, and apoptosis, a state also described in some models of cachexia. CD4$^+$ T-cell subset lymphopenia was measured in wasting and non-wasting diabetic mice. Our data show that the mechanism of wasting in diabetic mice involves muscle atrophy, a significant increase in ubiquitin conjugation, and upregulation of the ubiquitin ligases, muscle RING finger 1 (MuRF1) and muscle atrophy F box/atrogin-1 (MAFbx), indicating cachexia. Moreover, fragmentation of DNA isolated from atrophied muscle tissue indicates apoptosis. While CD4$^+$ T-cell lymphopenia is evident in all diabetic mice, CD4$^+$ T cells that express a very low density of CD44 were significantly lost in wasting, but not non-wasting, diabetic mice. These data suggest that CD4$^+$ T-cell subsets are not equally susceptible to cachexia-associated lymphopenia in diabetic mice.

Keywords: autoimmunity; cachexia; CD4/helper T cells; diabetes/insulin-dependent diabetes mellitus; immunodeficiency; lymphopenia

Introduction

Cachexia[1–5] is the dramatic weight loss and muscle atrophy seen in patients with cancer[1] and acquired immune deficiency syndrome (AIDS)[2] as well as in aging individuals[3,4] and in certain autoimmune conditions, including Type I diabetes (TID).[5] TID is an autoimmune disorder caused by the immune-mediated destruction of insulin-secreting pancreatic beta cells, resulting in low insulin production and high blood glucose levels.[6,7] Diabetes can be controlled with daily insulin injections. However, in the long term, diabetes leads to a variety of complications including muscle atrophy and cachexia.[5,8,9] Although significant progress has been made in the last decade towards understanding the pathways that lead to cachexia, the majority of these studies use models either of cancer cachexia, or of chemically induced diabetes. The availability of a model of TID cachexia will allow us to determine the relevance of previous studies to TID cachexia. Such a model will also allow further investigation of established pathways, and exploration of the possibility of novel pathways that are relevant to TID cachexia. In this study we describe the NOD mouse as a model for the study of TID cachexia.

Muscle atrophy in adults with TID,[5,8,9] and in rats with chemically induced diabetes,[10,11] as well as muscle atrophy in cancer cachexia,[1] involves significant muscle protein loss involving activation of the ubiquitin–proteasome

pathway.[12–15] Like patients with TID, the well-established non-obese diabetic (NOD) mouse, a model for spontaneous TID, is also susceptible to weight loss after diabetes onset.[16,17] The mechanism of wasting in the NOD mouse has not yet been reported.

Cachexia is characterized by muscle atrophy and a dramatic loss of muscle protein.[3,12–15] A significant loss in muscle DNA has also been described in some models, and this is associated with DNA fragmentation,[18,19] a classical apoptosis signature. Protein loss in cachexia is the result of a combination of active protein degradation and a decrease in protein synthesis.[14] Protein degradation involves activation of the ubiquitin–proteasome pathway[20] with an upregulation of the ubiquitin pathway-associated E3 ligases, muscle RING finger 1 (MuRF1) and muscle atrophy F box/atrogin-1 (MAFbx).[21]

An association between immunodeficiency and cachexia is evident in patients with AIDS,[22] in aging individuals,[23,24] and in individuals with autoimmunity.[25,26] Whether lymphopenia is a consequence of cachexia, or whether it plays an active role in the development of cachexia is not known. In the event that lymphopenia plays a role in promoting cachexia, then immune intervention might provide a novel therapeutic approach for the treatment of this syndrome. As a first approach in addressing this question we used the NOD mouse to determine whether the onset of cachexia was associated with the preferential loss of a particular $CD4^+$ immune cell subset.

A deficiency in $CD4^+$ T cells that express a low density of the cell surface marker CD44 ($CD44^{low}$) is associated with aging,[27,28] and with the development of spontaneous tumours.[29] CD44 is one of the cell surface markers used to distinguish antigen-inexperienced (naïve) from antigen-experienced (memory) $CD4^+$ T cells in the mouse. Naïve $CD4^+$ T cells express $CD44^{low}$ and a high density of CD62 ligand ($CD62L^{high}$), while memory cells express CD44 at a high density ($CD44^{high}$).[30,31] Naïve cells also express a high density of CD45RB ($CD45RB^{high}$).[32,33] By these criteria, the cell subset that is deficient in individuals with spontaneous tumours and during aging is a naïve $CD4^+$ T cell. Using these markers to distinguish naïve from memory $CD4^+$ T-cell subsets, we have tested the hypothesis that naïve $CD4^+$ T cells are more susceptible to cachexia-associated lymphopenia in diabetic mice than memory $CD4^+$ T cells.

Here we show that, like muscle atrophy in patients with TID, the mechanism of muscle atrophy in the NOD mouse also involves activation of the ubiquitin–proteasome pathway, suggesting the NOD mouse as a model for the study of TID-induced cachexia. In addition, we have extended these findings to show that cachexia in TID involves upregulation of both the MAFbx and MuRF1 E3 ligases. Although apoptosis was detected in skeletal muscle from wasting diabetic mice, it was only evident as a late event. Having established the NOD mouse as a model for TID cachexia we use it to show that both memory $CD4^+$ T cells and naïve $CD4^+$ T cells are lost in diabetic cachectic mice compared to non-diabetic mice. However, the only $CD4^+$ cell subset that is significantly lost between the onset of diabetes and the onset of cachexia, is the subset that expressed the lowest density of CD44 ($CD44^{v.low}$), suggesting that the loss of this cell subset is specific to the development of cachexia. Further investigation will be required to determine whether the loss of this cell subset promotes cachexia and whether inhibiting its loss might provide a novel therapeutic strategy for the treatment of this syndrome.

Materials and methods

Mice

Female NOD/LtJ (NOD) adult mice were purchased from the Jackson Laboratories (Bar Harbor, ME). In our vivarium 70–80% of female NOD mice become diabetic between 14 and 26 weeks of age.

Assessment of diabetes

Every week for the duration of the experiment, blood glucose levels (BGL) were tested using a one-step Bayer Glucometer Elite (Bayer, Elkhart, IN). Mice that had a BGL > 300 mg/dl were tested again 2 days later to confirm the high glucose level. Mice were considered diabetic when their BGL were > 300 mg/dl over two consecutive readings.

Assessment of wasting

Mice were weighed three times a week for the duration of the experiment and were considered to be wasting when their body weight was 20% less than at the beginning of the experiment. Weight loss in excess of 20% was associated with morbidity and mortality and therefore, wasting mice were killed and their tissues were taken for analysis within 24 hr of wasting assessment.

Measurement of food and water intake

Age-matched diabetic and non-diabetic NOD mice were housed one mouse per cage. Food weight (g) and water volume (ml) provided to each cage was measured over 24-hr periods every 2 days for the duration of the experiment. The effect of diabetes and wasting on food and water intake was determined.

Skeletal muscle protein isolation and quantification

The left and right gastrocnemius muscles were isolated, weighed, then individually wrapped in autoclaved alumin-

ium foil and stored at −80° until analysed. The packed gastrocnemius muscle was immersed in liquid nitrogen and ground with a mortar and pestle. The powdered tissue was transferred into 1 ml of ice-cold homogenization buffer [Tris–HCl 0·01 M, 2 mM ethylenediaminetetraacetic acid, 0·15 M NaCl, 0·012 M Brij 96, 2·22 mM nonidet P-40, 0·025 mM leupeptin, 0·025 mM aprotinin, 0·025 mM 4-(2-aminoethyl) benzenesulphonyl fluoride hydrochloride and homogenized with an electronic pellet pestle. The homogenates were incubated for 30 min at 4°, and centrifuged at 14 000 ***g*** for 10 min at 4°. Supernatants were thawed and diluted 1 : 800 in distilled H_2O on ice. Soluble protein concentration was determined by mixing 160 ml of the diluted sample with 40 ml of Bio-Rad dye reagent (Bio-Rad, Hercules, CA) in a 96-well plate using bovine serum albumin as the protein standard. Supernatant measurements were performed at least in duplicate. The plates were incubated for 10 min at room temperature and read at 595 nm on a microplate reader (Molecular Devices, Sunnyvale, CA).

Skeletal muscle DNA quantification and DNA fragmentation

The lateral and anterior thigh muscles were excised from both hind legs of each mouse and weighed. Tissue samples (50 mg) were minced and then lysed in a 6-M guanidinium chloride buffer containing proteinase K (40 μg/ml) at 55° for 2–4 hr and then treated briefly with DNase-free RNase following the DNeasy protocol (Qiagen, Valencia, CA). Before spin column treatment of lysates, small aliquots were diluted in 1 M urea for total DNA measurements using a fluorometric DNA assay[34] with Hoechst dye 33258 (Bio-Rad). Upon elution of genomic DNA from each spin column, samples were analysed on a 1·2% agarose gel in 1 × Tris–borate–EDTA buffer (TBE) containing ethidium bromide and digital images were recorded on an Eagle Eye II UV transilluminator system (Stratagene, La Jolla, CA). DNA was similarly isolated from liver tissue of mice treated with anti-Fas monoclonal antibody (mAb) (Jo2; Pharmingen, La Jolla, CA) for use as a positive control for DNA fragmentation.[35]

Ubiquitin conjugation by Western blot

Protein was isolated from gastrocnemius muscle samples as described above. Thirty-milligram samples of protein supernatant were fractionated by sodium dodecyl sulphate–polyacrylamide gel electrophoresis (4–20% gradient) and the separated proteins were then transferred onto 0·45-μm polyvinylidene fluoride membranes (Millipore, Billerica, MA). The membranes were blocked with 5% non-fat dried milk and then incubated with anti-ubiquitin polyclonal antiserum (1 : 100 dilution, Sigma-Aldrich, St Louis, MO) in 5% non-fat dried milk for 2 hr. The blots were washed three times and then incubated with a 1 : 5000 dilution of either horseradish peroxidase-conjugated, anti-rabbit immunoglobulin G (IgG-HRP; Bio-Rad), or anti-mouse IgG-HRP (Bio-Rad). After additional washes, the blots were developed with enhanced chemiluminescence (ECL) Western blotting detection reagents (Amersham, Piscataway, NJ), and captured on Hyperfilm ECL (Amersham). Ubiquitin-conjugated proteins appear as a smear rather than discrete bands.[36] Therefore, each lane was scanned and the intensity of the smear was analysed using IMAGE J version 1.36b (National Institutes of Health, Bethesda, MD).

MuRF1 and MAFbx measurements by reverse transcription–polymerase chain reaction (RT-PCR)

The gastrocnemius muscle was isolated in the presence of RNAlater RNA Stabilization Reagent (Qiagen). Total RNA was extracted from 50-mg aliquots of stabilized muscle using TRIzol Reagent (Sigma-Aldrich) according to the manufacturer's instructions. RNA samples were digested with RNase-free DNase I (Invitrogen, Carlsbad, CA) and RT-PCR were performed using Ready-to-go RT-PCR beads (GE Healthcare, Piscataway, NJ). Briefly, 2 mg RNA and 10 mM of the primers were added to the RT-PCR beads in diethylpyrocarbonate (DEPC) water, and the PCR mixtures were subjected to thermal cycling (Bio-Rad) as follows: 42° for 30 min for reverse transcription, followed by 95° for 5 min, 55° for 2 min, 72° for 2 min and 75° for 5 min. For all the amplified genes, primers were designed using the PRIMERS3 program, synthesized (Operon, Huntsville, AL) and used at a final concentration of 400 mM. The sequences for the primers were as follows: β-actin [400 base pairs (bp)]: 5′-TGGA ATCCTGTGGCATCCATGAAAC-3′ (forward) and 5′-TA AAACGCAGCTCAGTAACAGTCC-3′ (reverse); MuRF1 (573 bp): 5′-GTCCATGTCTGGAGGTCGTT-3′ (forward) and 5′-GTGGACTTTTCCAGCTGCTC-3′ (reverse); and MAFbx (845): 5′-GAACATCATGCAGAGGCTGA-3′ (forward) and 5′-CTTCTTGGCCTGCTGAAAAC-3′ (reverse). PCR products were separated on a 2% agarose gel containing ethidium bromide and gel images were visualized on a UV transilluminator and photographed (Alpha Innotech, San Leandro, CA). The intensity of the bands was quantified using IMAGE J version 1.36b.

Cell subset analysis

Spleen cells from 2- to 4-month-old female NOD mice were prepared for single-cell suspensions. Red blood cells were removed with lysing buffer (Sigma Chemical Co., St Louis, MO), and the remaining spleen cells were resuspended in phosphate-buffered saline with 1% fetal bovine serum (Intergen Co., New York, NY). Splenocytes were

labelled with an allophycocyanin- (APC) conjugated CD4-specific mAb (RM4-5) and phycoerythrin- (PE) conjugated CD44-specific mAb (IM7). APC-conjugated rat IgG2a and PE-conjugated rat IgG2b were used as isotype controls. In some experiments, as indicated in the Results section, cells were labelled with APC-conjugated CD4-specific mAb and with either (1) PE-conjugated CD44-specific mAb and fluorescein isothiocyanate- (FITC) conjugated CD3-specific mAb (hamster IgG, 145-2C11), (2) PE-conjugated CD44-specific mAb and FITC-conjugated CD25-specific mAb (rat IgM, OX-39), (3) PE-conjugated CD44-specific mAb and FITC-conjugated CD45RB-specific mAb (rat IgG2a, C363.16A), (4) PE-conjugated CD44-specific mAb and FITC-conjugated CD38-specific mAb (rat IgG2a, 90), or (5) FITC-conjugated CD44 with PE-conjugated CD62L (rat IgG2a, MEL-14). In each experiment the relevant fluorochrome-conjugated isotype controls were used to determine the profile of the positive population. All cell populations were sampled and analysed using a FACSCalibur with CELLQUEST version 3.3 software (Becton Dickinson Immunocytometry Systems, La Jolla, CA). All mAbs and isotype controls were purchased from Pharmingen (La Jolla, CA).

Statistical analysis

The statistical significance for the association of wasting with the loss of skeletal muscle weight, protein and DNA content, and $CD4^+$ T-cell subsets was assessed using the Mann–Whitney *U*-test.[37] The statistical significance of the association of DNA fragmentation, ubiquitin conjugation, E3 ligase upregulation and myosin heavy chain degradation with cachexia was determined using the unpaired *t*-test.[38] A linear correlation between the onset of diabetes and the onset of wasting was determined using the Spearman rank correlation.[39] A P value $\leq 0{\cdot}05$ was considered significant for all tests. The level of statistical significance is indicated on the figures as * for $P = 0{\cdot}05$ to $P = 0{\cdot}01$, ** for $P = 0{\cdot}009$ to $P = 0{\cdot}001$, *** for $P = 0{\cdot}0009$ to $P = 0{\cdot}0001$.

Results

NOD mice lose weight after diabetes onset

NOD female mice were monitored for diabetes and wasting from the age of 10 weeks. Of the 22 mice studied, 16 (74%) became diabetic between 14 and 25 weeks of age. Fourteen of the diabetic mice became wasting between 16 and 27 weeks of age (Fig. 1a). None of the non-diabetic mice became wasting, and those diabetic mice that were wasting did not lose weight until after the onset of diabetes (Fig. 1b). A linear correlation between the age at onset of diabetes and the age at onset of wasting was found to be highly significant ($P < 0{\cdot}0001$) with a correlation coefficient of 0·9877 and a 95% confidence interval of 0·9591–0·9963 (Fig. 1b), indicating that the mechanisms that result in onset of diabetes and onset of wasting are linked.

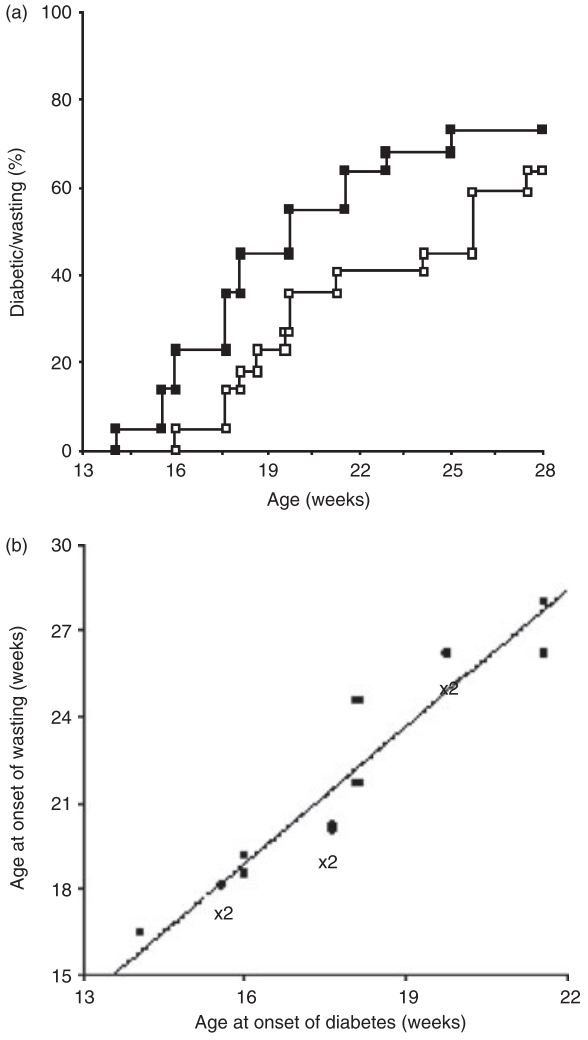

Figure 1. Non-obese diabetic (NOD) mice lose weight after diabetes onset. NOD female mice were monitored for the development of diabetes and wasting ($n = 22$). (a) The percentage of mice that were diabetic (closed squares) and wasting (open squares) over a 15-week period. (b) The relationship between age of diabetes onset and the age at onset of wasting. The closed circle indicates an individual diabetic mouse while the closed circle ×2 indicates two mice that became diabetic and wasting on the same day ($n = 14$). Using Spearman Rank Correlation the linear correlation between the age at onset of diabetes and the age at onset of wasting was found to be highly significant ($P < 0{\cdot}0001$) with a correlation coefficient of 0·9877 and a 95% confidence interval of 0·9591–0·9963. The data are pooled from two experiments.

Weight loss in diabetic NOD mice is not associated with a reduction in food and water intake

Mice that became diabetic between 14 and 16 weeks of age, and age-matched non-diabetic NOD mice were

housed separately in individual cages. All mice were weighed every 2–4 days. Four hundred millilitres water and 200 g food pellets were measured and given to each diabetic mouse on the day of the second high BGL reading indicating diabetes, and to an equal number of age-matched non-diabetic mice. The remaining food and water were measured for each cage 24 hr later. The procedure for measuring food and water intake was repeated every 2–4 days as indicated in Fig. 2. BGL for all mice was measured again at the end of the experiment to confirm the diabetic state of each animal. Only non-diabetic mice that remained non-diabetic for the duration of the experiment are shown as non-diabetic in Fig. 2. As previously shown in Fig. 1, wasting was evident in diabetic mice by 2–3 weeks after the onset of diabetes (Fig. 2a). Diabetic mice increased their food intake within the first 2 weeks after diabetes onset compared to non-diabetic mice. However, food intake was not significantly different in diabetic and non-diabetic mice during the period of weight loss (Fig. 2b). Water intake was also greater in diabetic mice compared to non-diabetic control mice, and this remained higher in diabetic mice than in non-diabetic mice during the period of weight loss (Fig. 2c).

Skeletal muscle is targeted in wasting NOD mice

NOD mice were monitored for wasting. Anterior lateral thigh and gastrocnemius muscles were removed from the lower limbs of mice that were either diabetic and wasting, or neither diabetic nor wasting, and weighed. The weights of both thigh and gastrocnemius muscles were significantly less in mice that were wasting than in mice that were not wasting, indicating muscle atrophy (Table 1). In addition, when compared to total body weight, skeletal muscle weight was preferentially reduced in wasting mice. This is shown in Table 1 by calculating the ratio of total body weight to skeletal muscle weight.

Wasting in NOD mice is associated with significant skeletal muscle protein and DNA loss

Cachexia is associated with significant skeletal muscle protein loss, and in some models, DNA loss. Therefore, we isolated skeletal muscle from mice that were wasting (and diabetic) and non-wasting (and not diabetic) and measured both protein and DNA content. Both were significantly reduced in skeletal muscle from wasting mice compared to non-wasting mice (Table 2). These data were consistent with the presence of muscle cachexia.

Skeletal muscle atrophy in NOD mice is associated with apoptosis

Loss of DNA in muscle cachexia has been associated with apoptosis in the muscle tissue.[18,19] Therefore, we directly tested the possibility that muscle atrophy in NOD mice was associated with apoptosis. Skeletal muscle was isolated from five wasting mice and nine

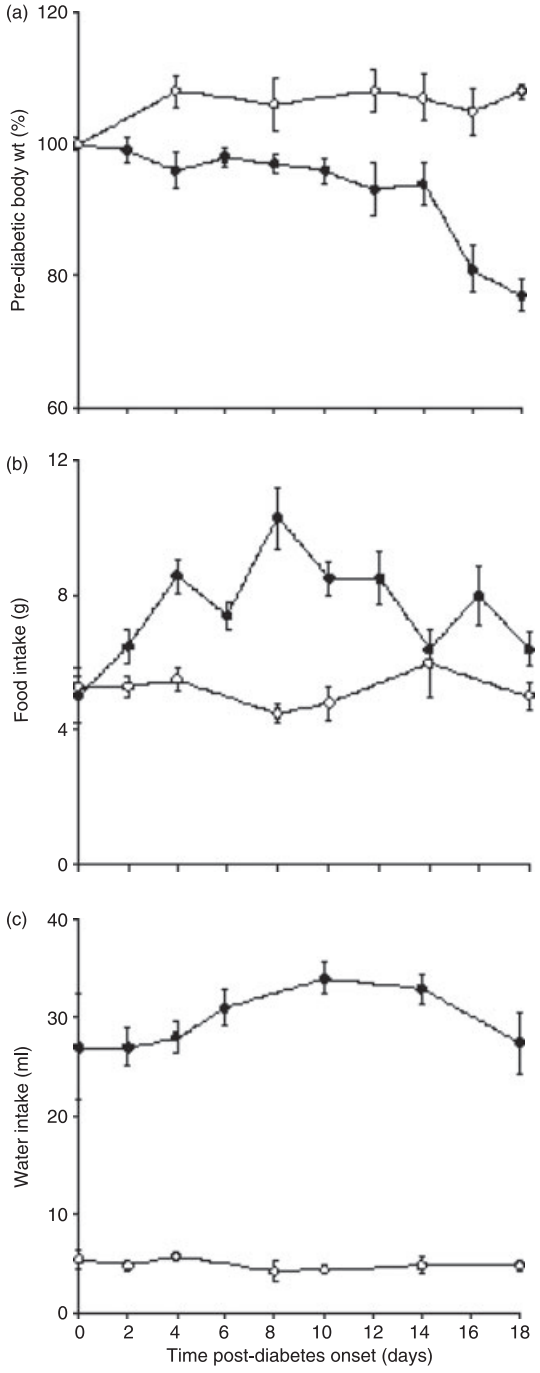

Figure 2. Weight loss in diabetic non-obese diabetic (NOD) mice is not associated with a reduction in food and water intake. Diabetic (closed circles, $n = 11$) and non-diabetic (open circles, $n = 9$) age-matched female NOD mice were monitored for (a) wasting, (b) food intake and (c) water intake. Data show the mean ± SEM for % of prediabetic body weight, food intake and water intake for diabetic mice after diabetes onset (closed circles). Measurements are taken at the same time for age-matched non-diabetic mice (open circles) for direct comparison.

Table 1. Skeletal muscle is preferentially targeted in wasting non-obese diabetic mice

	Wasting[1]	Non-wasting[2]	*P* value[3]
Total body weight (g)	17 ± 1·9[4]	23·9 ± 1·5	< 0·0001
Right gastrocnemius weight (mg)[5]	62·9 ± 15·7	117·6 ± 15·3	< 0·0001
Right thigh weight (mg)[5]	81·4 ± 12·2	155·8 ± 13·3	< 0·0001
Body weight : gastrocnemius weight[6]	284 ± 75	206 ± 31	0·001
Body weight : thigh weight[6]	212 ± 31	160 ± 18	< 0·0001

[1]Female diabetic non-obese diabetic mice were monitored for weight loss. Mice were considered wasting when their body weight was reduced by more than 20% ($n = 9$).
[2]Wasting mice were compared to age-matched non-wasting mice ($n = 14$). Non-wasting mice had lost between 0 and 5% body weight.
[3]The Mann–Whitney *U*-test was used to determine statistical significance between groups. A P value of $< 0·05$ was considered significant.
[4]The values given are the mean ± SD for each group.
[5]The tissue applies to the anterior and lateral thigh muscles isolated from both lower limbs of each mouse.
[6]The ratios of body weight : gastrocnemius weight and body weight : thigh weight were calculated by dividing the total body weight by the relevant muscle weight.

Table 2. Wasting in non-obese diabetic mice is associated with significant skeletal muscle protein and DNA loss

	Wasting[1]	Non-wasting[2]	*P* value[3]
Protein[4] (mg)	7·0 ± 1·6[5]	19·0 ± 3·4	0·02
DNA[6] (mg)	157 ± 34	295 ± 88	0·04
Protein : DNA	49 ± 14	67 ± 13	0·14

[1]Ten-week-old female non-obese diabetic mice were monitored for the development of wasting. Mice were considered wasting when their body weight was reduced by greater than 20% ($n = 8$). All mice that were wasting were also diabetic.
[2]Wasting mice were compared to age-matched non-wasting mice ($n = 7$). All of the non-wasting mice in this group were non-diabetic.
[3]The Mann–Whitney *U*-test was used to determine statistical significance between groups. A P value of $< 0·05$ was considered significant.
[4]Protein content of gastrocnemius muscle is shown.
[5]The values given are the mean ± SD for each group.
[6]DNA content of thigh muscle is shown.

non-wasting mice. DNA was isolated and DNA fragmentation was determined. Figure 3 shows representative samples of DNA from skeletal muscle of wasting and non-wasting mice. Muscle from all wasting mice showed DNA fragmentation while none of the muscles from non-wasting mice showed fragmentation ($P = 0·0005$). These data strongly suggest that skeletal muscle wasting in NOD mice involves apoptosis.

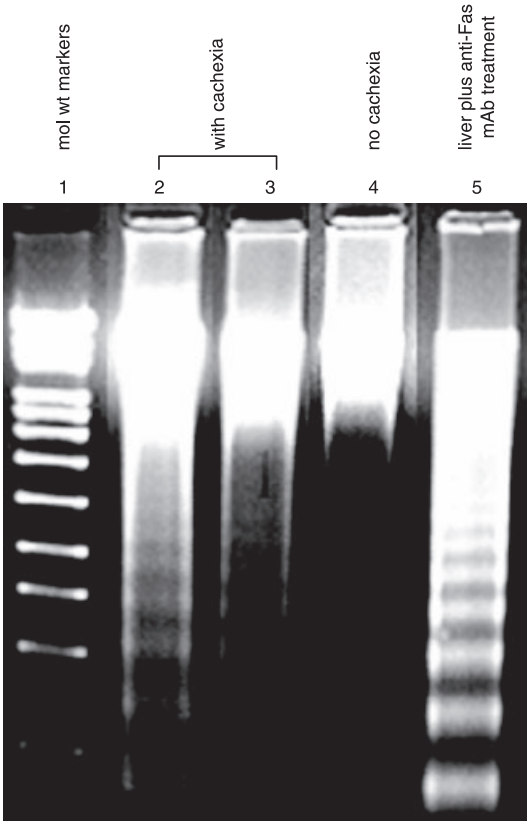

Figure 3. Cachexia in non-obese diabetic (NOD) mice is associated with apoptosis. Onset of wasting was monitored in female NOD mice from the age of 10 weeks to 18 weeks. Skeletal muscle from five wasting diabetic mice and nine non-wasting diabetic mice were analysed for evidence of apoptosis. The electrophoretic patterns of two representative samples of DNA from wasting mice (lanes 2 and 3, 24% and 20% weight loss respectively) and a single representative example of DNA from a non-wasting mouse (lane 4) are shown. The DNA ladder molecular weight markers and a positive control for apoptotic laddering are shown in lanes 1 and 5, respectively. The electrophoretic data are presented as a composite of lanes from the same gel. Using Fisher's exact test the data show a significant correlation between the presence of DNA laddering in mice that are wasting and the lack of DNA fragmentation in mice that are not wasting ($P = 0·0005$). The data are pooled from two experiments.

Significant skeletal muscle protein loss is associated with wasting and not diabetes without wasting

Data shown in Table 1 indicate that muscle atrophy in the wasting diabetic NOD mouse is associated with significant protein loss. To confirm that muscle protein was associated with wasting, and not with diabetes in the absence of wasting, skeletal muscle was isolated from mice that were either diabetic and wasting, or diabetic but not wasting, or neither diabetic nor wasting. Significant loss of soluble protein was only detected in muscle isolated from diabetic mice that were wasting and not from mice that were diabetic but not wasting (Fig. 4).

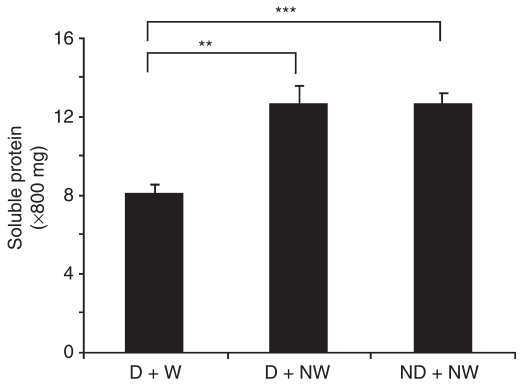

Figure 4. Significant skeletal muscle protein loss is associated with wasting and not with diabetes without wasting. Soluble protein extract was isolated from the gastrocnemius muscle of mice that were either, diabetic and wasting (D + W, $n = 6$), diabetic but not wasting (D + NW, $n = 7$), or not diabetic and not wasting (ND + NW, $n = 7$). Total soluble protein in each muscle was determined and the mean ± SEM was compared between groups. Data are pooled from two independent experiments. The level of statistical significance is indicated as * for $P = 0{\cdot}05$ to $P = 0{\cdot}01$, *** for $P = 0{\cdot}0009$ to $P = 0{\cdot}0001$.

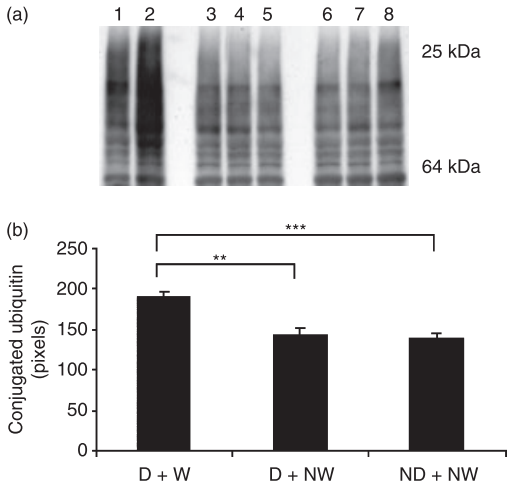

Figure 5. Muscle atrophy in diabetic mice is associated with a significant increase in ubiquitin conjugation. The extent of ubiquitin conjugation of protein in the gastrocnemius muscle of mice that were either, diabetic and wasting (D + W, $n = 6$), diabetic and non-wasting (D + NW, $n = 7$), or non-diabetic and non-wasting (ND + NW, $n = 7$) was determined. (a) Lanes 1 and 2 contain samples from two D + W mice, lanes 3–5 contain samples from three D + NW mice, and lanes 6–8 contain samples from three ND + NW mice. An equivalent amount of protein was loaded into each lane. The relative amount of ubiquitinated protein in muscle from each mouse was determined by measuring the number of pixels from 64 000 to 250 000 for each lane. (b) The mean ± SEM for the total pixel number per lane between 64 000 and 250 000 calculated for each group. Data are pooled from two independent experiments. The level of statistical significance is ** for $P = 0{\cdot}009$ to $P = 0{\cdot}001$, *** for $P = 0{\cdot}0009$ to $P = 0{\cdot}0001$.

Muscle atrophy in diabetic mice is associated with a significant increase in ubiquitin conjugation and the E3 ligase MuRF1, but not MAFbx

To determine whether protein ubiquitination is associated with muscle atrophy in diabetic NOD mice, the extent of protein conjugated to ubiquitin in skeletal muscle samples from either diabetic wasting mice, diabetic non-wasting mice, or non-diabetic non-wasting mice was compared (Fig. 5a). Ubiquitination of high molecular weight proteins (64 000–250 000) is significantly greater in diabetic mice that are wasting compared to diabetic mice that are not wasting (Fig. 5b). Ubiquitination of lower molecular weight proteins (22 000–64 000) was less than that for high-molecular-weight proteins, and was not significantly different between groups (data not shown).

The ubiquitin protein ligases MuRF1 (Fig. 6a) and MAFbx (Fig. 6b) were measured in skeletal muscle from mice in all three groups. Upregulation of MuRF1 was significantly increased at the onset of wasting, but not at the onset of diabetes (Fig. 6c). However, MAFbx upregulation was significantly greater in mice that were diabetic and wasting compared to mice that were non-diabetic and non-wasting, but not compared to mice that were diabetic but not wasting, suggesting that both diabetes and wasting play a role in MAFbx upregulation (Fig. 6d).

$CD4^{+/-}$ $CD44^{v.low}$ cell deficiency in cachectic mice

The expression of CD44 on $CD4^+$ splenocytes from non-diabetic (ND) and non-cachectic (NC) mice (Fig. 7a) was analysed in histogram format to define cell subsets by CD44 surface expression (very low, low, intermediate and high; Fig. 7b). By comparison, the CD44 expression profile from simultaneously diabetic (D) and cachectic (C) mice differed significantly (Fig. 7c), whereas the CD44 expression profile of mice that were diabetic but not cachectic was not different from that shown for non-diabetic mice (data not shown). Strikingly, in diabetic mice that became cachectic (D/C) there was a significant reduction in $CD4^+$ $CD44^{v.low}$ cells compared to non-cachectic mice that were either non-diabetic (ND/NC, $P = 0{\cdot}002$; Fig. 7d) or diabetic (D/NC, $P = 0{\cdot}008$; Fig. 7d). In addition, the total number of $CD4^+$ $CD44^{v.low}$ cells in non-cachectic mice was the same whether the mice were diabetic or not (Fig. 7d). These data suggest the possibility that a deficiency in $CD4^+$ $CD44^{v.low}$ cells in the spleen is associated with the development of cachexia but not diabetes.

The data were further analysed to determine whether cachexia was associated with a deficiency in total naïve $CD4^+$ ($CD44^{low}$) T cells. We found that the total number of $CD4^+$ $CD44^{low}$ cells ($CD4^+$ $CD44^{v.low}$ plus $CD4^+$ $CD44^{int}$) was not significantly reduced at the onset of diabetes when splenocytes from non-diabetic mice

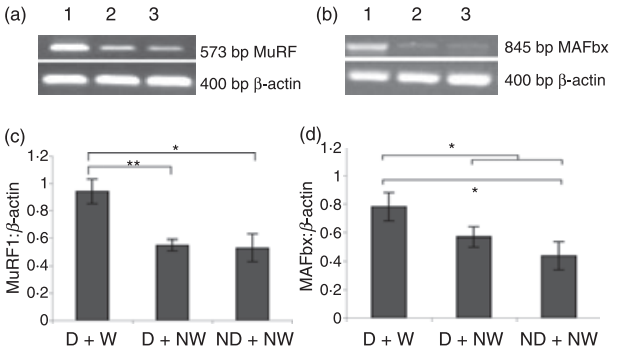

Figure 6. The E3 ligase muscle RING finger 1 (MuRF1) is significantly upregulated at the onset of wasting, while upregulation of muscle atrophy F box/atrogin-1 (MAFbx) requires both diabetes and wasting. The relative expression of MuRF1 and MAFbx in skeletal muscle from mice that were either diabetic and wasting (D + W, $n = 6$), diabetic but not wasting (D + NW, $n = 7$), or neither diabetic nor wasting (ND + NW, $n = 7$) was determined by semi-quantitative reverse transcription–polymerase chain reaction. β-Actin [400 base pairs (bp)] was used as an internal control. The expression of MuRF1 (a) and MAFbx (b) appear as single bands of 573 bp and 845 bp respectively. The relative expression of MuRF1 and MAFbx between groups was compared by determining the ratio of either MuRF1 or MAFbx to β-actin for each sample, and then comparing that ratio between groups. (a,b) Representative images of expression of either MuRF1, or MAFbx (top band) and β-actin (lower band) of mice with D+W (lane 1), D+NW (lane 2) and ND+NW (lane 3). The mean + SEM of the ratio of MuRF1 to β-actin (c), or MAFbx to β-actin (d) is shown for each group. The level of statistical significance is shown by * for $P = 0{\cdot}05$ to $P = 0{\cdot}01$, ** for $P = 0{\cdot}009$ to $P = 0{\cdot}001$.

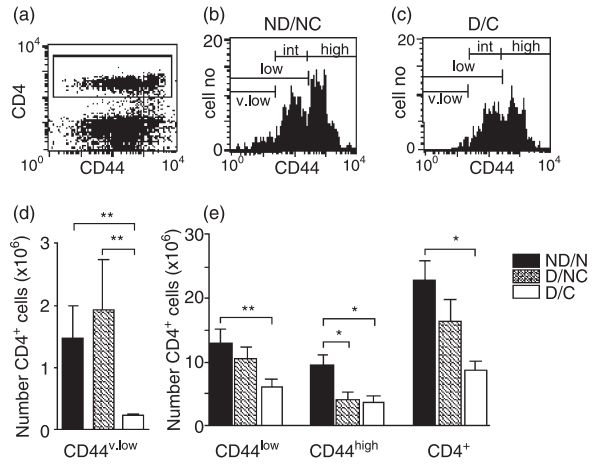

Figure 7. $CD4^{+/-}$ $CD44^{vLow}$ cells are deficient in cachexia. fluorescence-activated cell sorting profiles show the density of expression of CD44 on $CD4^+$ splenocytes from representative examples of (a,b) non-diabetic and non-cachectic mice (ND/NC) and (c) diabetic and cachectic mice (D/C). The mean number of $CD4^+$ cells (± SEM) that express CD44 at either (d) a very low ($CD44^{v.low}$) density or (e) at a low ($CD44^{low}$) or high ($CD44^{high}$) density, in non-diabetic and non-cachectic (closed bars, ND/NC, $n = 5$), diabetic and non-cachectic (hatched bars, D/NC, $n = 5$) and diabetic and cachectic (open bars, D/C, $n = 5$) mice is shown. The mean ± SEM of the total number of $CD4^+$ cells in each group is also shown in (e). The level of statistical significance is indicated as * for $P = 0{\cdot}05$ to $P = 0{\cdot}01$ and ** for $P = 0{\cdot}009$ to $P = 0{\cdot}001$. The data are representative of three experiments.

(ND/NC) were compared to splenocytes from diabetic mice (D/NC). In contrast, at the onset of cachexia (D/C) there was a significant reduction in the number of both $CD4^+$ $CD44^{low}$ and total $CD4^+$ splenocytes compared to splenocytes from non-diabetic mice (Fig. 7e; $P = 0{\cdot}008$ and $P = 0{\cdot}01$, respectively). Analysis of the memory $CD4^+$ T-cell population showed that the total number of $CD4^+$ $CD44^{high}$ cells in spleens of cachectic mice was significantly reduced in non-cachectic diabetic mice compared to non-diabetic mice, suggesting an association between memory cell deficiency and the onset of diabetes ($P = 0{\cdot}03$, Fig. 7e). However, a further reduction in the number of memory cells was not detected in the spleens of mice that were also cachectic (D/C) compared to the spleens of diabetic mice that were not cachectic (D/NC).

The phenotype of $CD4^{+/-}$ $CD44^{v.low}$ cells

To determine whether $CD4^+$ $CD44^{v.low}$ cells could be distinguished from naïve $CD4^+$ T cells phenotypically, NOD splenocytes were colabelled with mAb-specific CD4 and CD44 (Fig. 8a), and for additional cell surface markers that distinguish $CD4^+$ T-cell subsets. The data shown in Fig. 8 indicate that, like naïve $CD4^+$ T cells, the

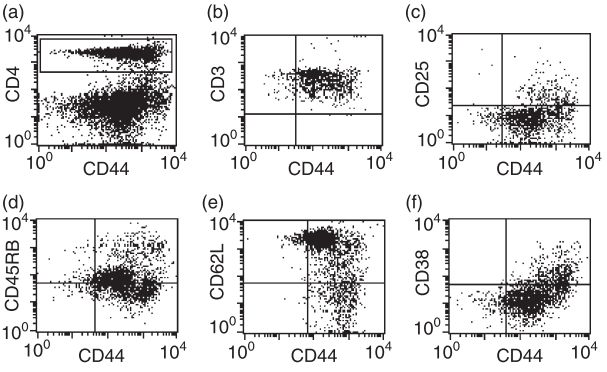

Figure 8. The phenotype of CD4± $CD44^{v.low}$ cells. Splenocytes from 10-week-old non-obese diabetic (NOD) female mice were labelled with CD4-specific and CD44-specific antibodies in combination with antibodies specific for one of CD3 ($n = 8$), CD25 ($n = 12$), CD45RB ($n = 8$), CD62L ($n = 8$) or CD38 ($n = 8$). Data shown in (a) are representative of the coexpression of CD44 and CD4 on NOD splenocytes. Data shown in (b–f) are representative of the co-expression of CD44 and either CD3 (b), CD25 (c), CD45RB (d), CD62L (e) or CD38 (f) on $CD4^+$ cells in four separate experiments. The horizontal bars are set based on the isotype control profiles. $CD4^+$ $CD44^{v.low}$ cells are to the left of the vertical bars in each panel.

$CD4^+$ $CD44^{v.low}$ cells were $CD3^+$ as expected (Fig. 8b), they did not express the regulation/activation marker CD25 (Fig. 8c), they expressed a mixture of intermediate- and high-density CD45RB (Fig. 8d), were $CD62L^{high}$ (Fig. 8e), and did not express CD38 (Fig. 8f).

Discussion

One of the long-term complications in patients with TID,[5,8,9] and in chemically-induced diabetes in the rat,[10,11,40,41] is muscle atrophy caused by accelerated proteolysis. In this study we find that wasting in the diabetic NOD mouse, the well-characterized mouse model for spontaneous TID, is also associated with profound skeletal muscle atrophy and a significant loss of skeletal muscle protein and DNA. Activation of the ubiquitin–proteasome pathway is shown by an increase in ubiquitin conjugation of high-molecular-weight proteins, and upregulation of both MAFbx and MuRF1 in skeletal muscle of wasting diabetic mice. Preferential ubiquitination of high-molecular-weight proteins has been reported in models of cancer,[42] starvation,[43] and cirrhosis,[44] and *in vitro* studies show that high-molecular-weight proteins are preferentially degraded by the proteasome complex.[43] Taken together, these data indicate that wasting in the diabetic NOD mouse involves cachexia.

Our data also show that a significant deficiency in the $CD4^+$ $CD44^{v.low}$ T-cell subset is associated with cachexia in diabetic mice, but not in diabetic mice in the absence of cachexia. $CD4^+$ $CD44^{v.low}$ T-cell deficiency might be caused either by cell death, or by differentiation to become $CD4^+$ $CD44^{int}$ and $CD4^+$ $CD44^{high}$ cells. The preferential loss of $CD4^+$ $CD44^{v.low}$ T cells rather than the equivalent loss of all $CD4^+$ T cells suggests either an increased susceptibility of $CD4^+$ $CD44^{v.low}$ T cells to cachexia-induced depletion compared to other $CD4^+$ cell subsets, or a role for $CD4^+$ $CD44^{v.low}$ T cells in preventing cachexia, resulting in a temporal association between their loss and the onset of cachexia. Further investigation will be required to distinguish between these possibilities.

The coexpression of a high density of CD62L and a mixture of intermediate and high expression of CD45RB, in addition to the low expression of CD44, suggests that the $CD4^+$ $CD44^{v.low}$ cells are naïve $CD4^+$ T cells. In addition, the lack of expression of the activation markers CD25[45] and CD38[46] is consistent with the notion that the $CD4^+$ $CD44^{v.low}$ cell subset described here is a resting naïve T-cell subset. Both CD25[47–49] and CD38[50] have also been described as markers that distinguish $CD4^+$ cell subsets with regulatory activity in the NOD mouse, suggesting that $CD4^+$ $CD44^{v.low}$ cells are not such regulatory cells, and this is also consistent with a naïve cell phenotype. In contrast to the $CD4^+$ $CD44^{v.low}$ cells, the naïve $CD4^+$ T-cell subset as a whole, $CD4^+$ $CD44^{low}$ cells, are not significantly reduced at the onset of cachexia in diabetic mice, although they are significantly reduced in cachectic mice when compared to mice that are neither cachectic nor diabetic, suggesting a continuous loss of this cell subset after the onset of diabetes. Memory $CD4^+$ T cells, on the other hand, are lost at the onset of diabetes and not at the onset of cachexia. Taken as a whole these data suggest that $CD4^+$ T-cell lymphopenia in the spleens of cachectic mice is not random, but that the $CD4^+$ $CD44^{v.low}$ cell subset is preferentially targeted.

Activation of the ubiquitin–proteasome pathway is common to cachexia seen under a variety of primary disease states, including cancer, chronic infection, diabetes, and starvation,[13,51] and has become the hallmark that defines wasting as cachexia. The ubiquitin protein E3 ligases, MuRF1 and MAFbx play a critical role in protein degradation by the proteasome pathway.[21] In the NOD mouse we find that whereas MuRF1 is significantly upregulated in the skeletal muscle of diabetic wasting mice compared to diabetic non-wasting mice, in the case of MAFbx upregulation, significance is only reached when diabetic and wasting mice are compared to non-diabetic and non-wasting mice. These data might suggest that MAFbx upregulation might begin in diabetic mice before wasting, and then continue as wasting proceeds.

The presence of DNA fragmentation indicates that TID-induced cachexia in the NOD mouse involves apoptosis of skeletal muscle cells. Although evidence of apoptosis has been described in cancer cachexia,[18,19,52] it has not been reported in chemically-induced diabetic rats.[53] Insulin-like growth factor-1 (IGF-1), a protein that is significantly reduced both in human TID[54] and in the diabetic NOD mouse,[55] inhibits caspase 3-mediated apoptosis.[56] Therefore, it is tempting to speculate that the mechanism for TID-induced cachexia involves apoptosis by a mechanism that involves a deficiency in IGF-1, and that the NOD model of cachexia provides a model to study mechanisms of apoptosis that are specific to TID cachexia.

A number of factors that play a causal role in the development of diabetes also play a causal role in the onset of cachexia. Insulin can therefore inhibit proteolysis by blocking ubiquitin-mediated proteasomal activity.[57] Moreover, treatment of patients with TID with insulin can inhibit protein breakdown.[8,58] However, although treatment with insulin stimulates weight gain in cachectic cancer patients, lean tissue mass was unaffected,[59] suggesting that the pathways that lead to cachexia in different primary disease states do not entirely overlap. In addition, reduced IGF-1 prevents protein breakdown[15] by abrogating proteasome activity in skeletal muscle.[60] Activation of the ubiquitin–proteasomal pathway in the diabetic NOD mouse might also be stimulated by the proinflammatory cytokines tumour necrosis factor-α and interferon-γ, which are upregulated during diabetes development,[61–63] and have been shown to stimulate the

activation of the ubiquitin proteasomal pathway leading to protein breakdown.[20] It is likely that protein breakdown in skeletal muscle of wasting diabetic mice is stimulated by a combination of factors that merge in their action to promote proteolysis and apoptosis.

To our knowledge, this is the first report that shows that wasting in the NOD mouse model of spontaneous TID is the result of cachexia. In addition, we show that the mechanism of cachexia in TID involves upregulation of the E3 ligases, MuRF1 and MAFbx. Moreover, like some, but not all, models of cancer cachexia, the mechanism of cachexia in TID also involves apoptosis. These findings suggest that the NOD mouse can be used as a model system to study multiple pathways in the development of TID-induced cachexia. Data generated from experiments designed to distinguish lymphopenia that is associated with diabetes onset, from lymphopenia that is associated with onset of cachexia, suggest that cachexia-associated $CD4^+$ T-cell lymphopenia is specific to the $CD4^+$ $CD44^{v.low}$ cells. Additional investigation will be required to determine whether these cells are a functionally distinct $CD4^+$ T-cell subset, and whether their loss is an effect of cachexia, or whether the loss of this cell subset plays a role in causing cachexia. In the long term we hope that a better understanding of the mechanisms that lead to cachexia in TID, including a clear evaluation of the potential role for $CD4^+$ $CD44^{v.low}$ cells, will lead to novel therapeutic strategies for the treatment of cachexia in patients with TID.

Acknowledgements

Funding for this study was provided by grants from the Diabetes National Research Group (DNRG0603), the Alzheimer's and Ageing Research Center (AARC5104), and the National Institutes of Health (DK61334 and CA109729) to Joanna Davies. We would like to thank Dr Donna McCarthy for valuable discussions during the execution of this study.

References

1 Donnelly S, Walsh D. The symptoms of advanced cancer. *Semin Oncol* 1995; **22**:67–72.
2 Strawford A, Hellerstein M. The etiology of wasting in the human immunodeficiency virus and acquired immunodeficiency syndrome. *Semin Oncol* 1988; **25**:76–81.
3 Grounds MD. Reasons for the degeneration of ageing skeletal muscle: a central role for IGF-1 signalling. *Biogerontology* 2002; **3**:19–24.
4 Wallace JI, Schwartz RS. Epidemiology of weight loss in humans with special reference to wasting in the elderly. *Int J Cardiol* 2002; **85**:15–21.
5 Nair KS, Ford GC, Ekberg K, Fernqvist-Forbes E, Wahren J. Protein dynamics in whole body and in splanchnic and leg tissues in type I diabetic patients. *J Clin Invest* 1995; **95**:2926–37.
6 Castano L, Eisenbarth GS. Type-I diabetes: a chronic autoimmune disease of human, mouse and rat. *Annu Rev Immunol* 1990; **8**:647–79.
7 Tisch R, McDevitt H. Insulin-dependent diabetes mellitus. *Cell* 1996; **85**:291–7.
8 Charlton M, Nair KS. Protein metabolism in insulin-dependent diabetes mellitus. *J Nutr* 1998; **128**:323S–7S.
9 Vogiatzi MG, Nair KS, Beckett PR, Copeland KC. Insulin does not stimulate protein synthesis acutely in prepubertal children with insulin-dependent diabetes mellitus. *J Clin Endocrinol Metab* 1997; **82**:4083–7.
10 Liu Z, Miers WR, Wei L, Barrett EJ. The ubiquitin–proteasome proteolytic pathway in heart vs skeletal muscle: effects of acute diabetes. *Biochem Biophys Res Commun* 2000; **276**:1255–60.
11 Merforth S, Osmers A, Dahlmann B. Alterations of proteasome activities in skeletal muscle tissue of diabetic rats. *Mol Biol Rep* 1999; **26**:83–7.
12 Price SR, Mitch WE. Mechanisms stimulating protein degradation to cause muscle atrophy. *Curr Opin Clin Metab Care* 1998; **1**:79–83.
13 Tisdale MJ. The ubiquitin–proteasome pathway as a therapeutic target for muscle wasting. *J Support Oncol* 2005; **3**:209–17.
14 Morley JE, Thomas DR, Wilson MM. Cachexia: pathophysiology and clinical relevance. *Am J Clin Nutr* 2006; **83**:735–43.
15 Delafontaine P, Akao M. Angiotensin II as candidate of cardiac cachexia. *Curr Opin Clin Nutr Metab Care* 2006; **9**:220–4.
16 Kikutani H, Makino S. The murine autoimmune diabetes model: NOD and related strains. *Adv Immunol* 1992; **51**:285–322.
17 Makino S, Kunimoto K, Muraoka Y, Mizushima Y, Katagiri K, Tochino Y. Breeding of a non-obese, diabetic strain of mice. *Jikken Dobutsu* 1980; **29**:1–213.
18 van Royen M, Carbo N, Busquets S, Alvarez B, Quinn LS, López-Soriano FJ, Argilés JM. DNA fragmentation occurs in skeletal muscle during tumor growth: a link with cancer cachexia? *Biochem Biophys Res Commun* 2000; **270**:533–7.
19 Carbo N, Busquets S, van Royen M, Alvarez B, Lopez-Soriano FJ, Argiles JM. TNF-alpha is involved in activating DNA fragmentation in skeletal muscle. *Br J Cancer* 2002; **86**:1012–6.
20 Mitch WE, Goldberg AL. Mechanisms of muscle wasting. The role of the ubiquitin–proteasome pathway. *N Engl J Med* 1996; **335**:1897–905.
21 Bodine SC, Latres E, Baumhueter S *et al.* Identification of ubiquitin ligases required for skeletal muscle atrophy. *Science* 2001; **294**:1704–8.
22 McMichael AJ, Rowland-Jones SL. Cellular immune responses to HIV. *Nature* 2001; **410**:980–7.
23 Chakravarti B, Abraham GN. Aging and T-cell-mediated immunity. *Mech Ageing Dev* 1999; **108**:183–206.
24 Burns EA, Goodwin JS. Immunodeficiency of aging. *Drugs Aging* 1997; **11**:374–97.
25 Jonsson R, Brokstad KA, Hansen T, Davies T, Ulvestad E. The evolution and breakdown of the immune system: implications for development of autoimmune diseases. *Scand J Immunol* 2002; **56**:323–6.
26 Jaramillo A, Gill BM, Delovitch TL. Insulin dependent diabetes mellitus in the non-obese diabetic mouse: a disease mediated by T cell anergy? *Life Sci* 1994; **55**:1163–77.
27 Barrat F, Haegel H, Louise A, Vincent-Naulleau S, Boulouis HJ, Neway T, Ceredig R, Pilet C. Quantitative and qualitative

changes in CD44 and MEL-14 expression by T cells in C57BL/6 mice during aging. *Res Immunol* 1995; **146**:23–34.
28 Timm JA, Thoman ML. Maturation of $CD4^+$ lymphocytes in the aged microenvironment results in a memory-enriched population. *J Immunol* 1999; **162**:711–7.
29 Miller RA, Turke P, Chrisp C *et al.* Age-sensitive T cell phenotypes covary in genetically heterogenous mice and predict early death from lymphoma. *J Gerontol* 1994; **49**:255–62.
30 Budd RC, Cerottini JC, Horvath C, Bron C, Pedrazzini T, Howe RC, MacDonald HR. Distinction of virgin and memory T lymphocytes: stable acquisition of the Pgp-1 glycoprotein concomitant with antigenic stimulation. *J Immunol* 1987; **138**:3120–9.
31 Swain SL. Generation and *in vivo* persistence of polarized Th1 and Th2 memory cells. *Immunity* 1994; **1**:543–52.
32 Bottomly K, Luqman M, Greenbaum L, Carding S, West J, Pasqualini T, Murphy DB. A monoclonal antibody to murine CD45R distinguishes CD4 T cell populations that produce different cytokines. *Eur J Immunol* 1989; **19**:617–23.
33 Lee WT, Yin XM, Vitetta ES. Functional and ontogenic analysis of murine $CD45R^{hi}$ and $CD45R^{lo}$ $CD4^+$ T cells. *J Immunol* 1990; **144**:3288–95.
34 Downs TR, Wilfinger WW. Fluorometric quantification of DNA in cells and tissue. *Anal Biochem* 1983; **131**:538–47.
35 Ogasawara J, Watanabe-Fukunaga R, Adachi M *et al.* Lethal effect of the anti-Fas antibody in mice. *Nature* 1993; **364**:806–9.
36 Minnaugh EG, Bonvini P, Neckers L. The measurement of ubiquitin and ubiquitinated proteins. *Electrophoresis* 1999; **20**:418–28.
37 Krauth J. The interpretation of significance tests for independent and dependent samples. *J Neurosci Methods* 1983; **9**:269–81.
38 Ludbrook J, Dudley H. Issues in biomedical statistics: analysing 2×2 tables of frequencies. *Aust N Z J Surg* 1994; **64**:780–7.
39 Gaddis ML, Gaddis GM. Introduction to biostatistics: Part 6, correlation and regression. *Ann Emerg Med* 1990; **19**:1462–8.
40 Price SR, Bailey JL, Wang X, Jurkovitz C, England BK, Ding X, Phillips LS, Mitch WE. Muscle wasting in insulinopenic rats results from activation of the ATP-dependent, ubiquitin–proteasome proteolytic pathway by a mechanism including gene transcription. *J Clin Invest* 1996; **98**:1703–8.
41 Pepato MT, Migliorini RH, Goldberg AL, Kettelhut IC. Role of different proteolytic pathways in degradation of muscle protein from streptozotocin-diabetic rats. *Am J Physiol* 1996; **271**:E340–7.
42 Combaret L, Tilignac T, Claustre A, Voisin L, Taillandier D, Obled C, Tanaka K, Attaix D. Torbafylline (HWA 448) inhibits enhanced skeletal muscle ubiquitin-proteasome-dependent proteolysis in cancer and septic rats. *Biochem J* 2002; **361**:185–92.
43 Wing SS, Haas AL, Goldberg AL. Increase in ubiquitin–protein conjugates concomitant with the increase in proteolysis in rat skeletal muscle during starvation and atrophy denervation. *Biochem J* 1995; **307**:639–45.
44 Lin S-Y, Chen W-Y, Lee F-Y, Huang C-J, Sheu WH-H. Activation of ubiquitin–proteasome pathway is involved in skeletal muscle wasting in a rat model with biliary cirrhosis: potential role of TNF-α. *Am J Physiol Endocrinol Metab* 2005; **288**:493–501.
45 Waldmann TA. The multi-subunit interleukin-2 receptor. *Annu Rev Biochem* 1989; **58**:875–911.
46 Jackson DG, Bell JI. Isolation of a cDNA encoding the human CD38 (T10) molecule, a cell surface glycoprotein with an unusual discontinuous pattern of expression during lymphocyte differentiation. *J Immunol* 1990; **144**:2811–5.
47 Shevach EM. $CD4^+$ $CD25^+$ suppressor T cells: more questions than answers. *Nat Rev Immunol* 2002; **2**:389–400.
48 Salomon B, Lenschow DJ, Rhee L, Ashourian N, Singh B, Sharpe A, Bluestone JA. B7/CD28 costimulation is essential for the homeostasis of the $CD4^+CD25^+$ immunoregulatory T cells that control autoimmune diabetes. *Immunity* 2000; **12**:431–40.
49 Pop SM, Wong CP, He Q, Wang Y, Wallet MA, Goudy KS, Tisch R. The type and frequency of immunoregulatory CD4+ T-cells govern the efficacy of antigen-specific immunotherapy in nonobese diabetic mice. *Diabetes* 2007; **56**:1395–402.
50 Martins TC, Aguas AP. A role for $CD45RB^{low}$ $CD38^+$ T cells and costimulatory pathways of T-cell activation in protection of non-obese diabetic (NOD) mice from diabetes. *Immunology* 1999; **96**:600–5.
51 Williams A, Sun X, Fischer JE, Hasselgren PO. The expression of genes in the ubiquitin–proteasome proteolytic pathway is increased in skeletal muscle from patients with cancer. *Surgery* 1999; **126**:744–9.
52 Smith HJ, Tisdale MJ. Induction of apoptosis by a cachectic-factor in murine myotubes and inhibition by eicosapentaenoic acid. *Apoptosis* 2003; **8**:161–9.
53 Lecker SH, Jagoe RT, Gilbert A *et al.* Multiple types of skeletal muscle atrophy involve a common program of changes in gene expression. *FASEB J* 2004; **18**:39–51.
54 Capoluongo E, Pitocco D, Santonocito C *et al.* Association between serum free IGF-I and IGFBP-3 levels in type-I diabetes patients affected with associated autoimmune diseases or diabetic complications. *Eur Cytokine Netw* 2006; **17**:167–74.
55 Landau D, Segev Y, Eshet R, Flyvbjerg A, Phillip M. Changes in the growth hormone-IGF-I axis in non-obese diabetic mice. *Int J Exp Diabetes Res* 2000; **1**:9–18.
56 Song YH, Li Y, Du J, Mitch WE, Rosenthal N, Delafontaine P. Muscle-specific expression of IGF-1 blocks angiotensin II-induced skeletal muscle wasting. *J Clin Invest* 2005; **115**:451–8.
57 Bennett RG, Hamel FG, Duckworth WC. Insulin inhibits the ubiquitin-dependent degrading activity of the 26S proteasome. *Endocrinology* 2000; **141**:2508–17.
58 Abu-Lebdeh HS, Nair KS. Protein metabolism in diabetes mellitus. *Baillieres Clin Endocrinol Metab* 1996; **10**:589–601.
59 Lundholm K, Korner U, Gunnebo L, Sixt-Ammilon P, Fouladiun M, Daneryd P, Bosaeus I. Insulin treatment in cancer cachexia: effects on survival, metabolism, and physical functioning. *Clin Cancer Res* 2007; **13**:2699–706.
60 Chrysis D, Zhang J, Underwood LE. Divergent regulation of proteasomes by insulin-like growth factor I and growth hormone in skeletal muscle of rats made catabolic with dexamethasone. *Growth Horm IGF Res* 2002; **12**:434–41.
61 McKenzie MD, Dudek NL, Mariana L, Chong MM, Trapani JA, Kay TW, Thomas HE. Perforin and Fas induced by IFNgamma and TNFalpha mediate beta cell death by OT-I CTL. *Int Immunol* 2006; **18**:837–46.
62 Skarsvik S, Tiittanen M, Lindstrom A, Casas R, Ludvigsson J, Vaarala O. Poor *in vitro* maturation and pro-inflammatory cytokine response of dendritic cells in children at genetic risk of type 1 diabetes. *Scand J Immunol* 2004; **60**:647–52.
63 Ng WY, Thai AC, Lui KF, Yeo PP, Cheah JS. Systemic levels of cytokines and GAD-specific autoantibodies isotypes in Chinese IDDM patients. *Diabetes Res Clin Pract* 1999; **43**:127–35.